A99-31075

AIAA 99-2218

A Practical Mechanism for Computing Combustion in Gas Turbine Engines

K.P. Kundu
P.F. Penko
T.J VanOverbeke
NASA Glenn Research Center
Cleveland, Ohio

35th AIAA/ASME/SAE/ASEE Joint Propulsion Conference and Exhibit
20–24 June 1999
Los Angeles, California

AIAA 99-2218

A Practical Kinetic Mechanism for Computing Combustion in Gas Turbine Engines

Krishna P. Kundu
Paul F. Penko
Thomas J. VanOverbeke
The NASA Glenn Research Center
Cleveland, Ohio

Abstract

Modifications to a 16-species, 23-step mechanism previously postulated for combustion of propane and Jet-A fuel in air are presented. The modifications remove dependency of the global reaction rate on process pressure. The mechanism is tested on three pressurized combustion case: 1) A premixed gaseous propane burner, 2) A single fuel-module burning liquid Jet-A fuel, and 3) An annular combustor burning liquid Jet-A fuel. The first two cases are experimental configurations. The first case has gas-sample emission data. The second case has PLIF measurements of OH concentrations in the near-field of the module exit surface. Comparisons of computed results are made with the experimental measurements to validate the chemical kinetics model. The third case is to demonstrate utility of the code with the kinetic set and a Reynolds-stress, turbulent-transport model for analyzing a combustor on a UNIX workstation.

Introduction

Jet-A, the fuel that commercial aircraft burn, is a mixture that spans a fairly wide range of light to heavy hydrocarbons. Because of the complexity and variation in its composition, the calculation of combustion reactions and product concentrations is usually an approximation. Generally, there are two types of approximate mechanisms used in combustion modeling and analysis: 1) Skeletal or simplified reaction mechanisms[1] and 2) Systematically reduced reaction mechanisms.[2] Skeletal mechanisms are simple, usually consisting of only a few reactions, are easily understood and readily applied in computational combustion codes. On the other hand, systematically reduced mechanisms[3] use more complex algebraic expressions, but so far are not widely used in numerical calculations because of difficulties associated with their complexity, namely storage limitations, matrix stiffness and CPU time.

For estimating emissions from burning Jet-A, it is desirable to calculate concentrations of the pollutant species produced. Here, we are particulary interested in the major pollutants, namely nitric oxide (NO) and carbon monoxide (CO). The well-known Zeldovich mechanism has long been used to calculate the NO formation that is time dependent and commonly called the "thermal NOx." The Zeldovich mechanism is often used in post-processing of a combustion flow field, using the temperature that is produced from a skeletal mechanism. With the trend toward increasingly lean combustion, the NO formed via the N_2O mechanism becomes a higher percentage of the total NO produced. The Zeldovich mechanism does not describe this formation.

One of the more difficult problems in developing a chemistry model for CFD is incorporating the appropriate ignition delay. This delay depends on a number of parameters, but primarily on fuel-air ratio, initial air temperature and pressure. These dependencies are usually too complex for a simple chemistry model to describe. In practical terms, ignition in most gas turbines is induced by a spark igniter. It is, therefore, not necessary to describe the pyrolysis-ignition process per se for quasi-steady combustion. This suggests that the ignition phase can be separated from the quasi-steady combustion phase and modeled by a physical process other than chemical kinetics. This effect is usually achieved numerically by simply adding internal energy to the flow, simulating an electrical spark.

In prior papers[6,10] we postulated two reduced mechanisms: 1) A 12-species mechanism with 13-reaction steps, and 2) A 16-species mechanism with 23-reaction steps. The basic premise in developing the mechanisms is that Jet-A behaves the same as propane once the fuel breaks down, by pyrolysis, into simpler hydrocarbon fragments. It further assumes that pyrolysis can be adequately described in a single, global reaction. This is an important feature toward simplification of the chemistry. Ignoring the pyrolysis steps makes the combustion calculations much faster and the burden on computer memory considerably less compared to schemes that employ detailed kinetic models or even reduced kinetic models that still have a considerable number of species and reaction steps for simulating pyrolysis. The mechanisms produced are based on propane combustion for the practical reason that they can be readily compared to established detailed mechanisms for propane. Proven detailed mechanisms are not available for Jet-A.

Though a small mechanism is often preferred for the usual numerical-computer reasons, we prefer the larger, moderately complex 16-species mechanism for the sake of more stable behavior of the CFD code and the ability to compute directly the pollutant concentrations. In this paper, we discuss modifications to this mechanism that eliminate the pressure dependency of the rate constant in the first, global reaction that simulates pyrolysis. Adjustment of this constant was required to handle different combustion pressure levels. We then demonstrate the use of the mechanism in three cases: 1) An experimental, premixed propane burner in a pressurized flametube with gas-sample NO measurements, 2) An experimental, Jet-A liquid fuel-spray, injector-swirler module in a pressurized combustor facility with PLIF measurements of OH concentrations, and 3) A hypothetical, annular combustor configuration with liquid Jet-A fuel injection. The last case is primarily intended to illustrate utility of the mechanism, in combination with a Reynolds-stress transport model for turbulence, on a UNIX workstation.

It should be noted that the model, via the computer code used, does not capture the interaction of fluid turbulence and chemical reactions on the fine, Kolmogorov scale. Rather, the chemical reactions only affect the flow through temperature and the resulting density and velocities. Furthermore, the intermittency of mixing, often present in the near-field of a fuel spray, is not considered, other than through the interaction of the stochastic spray model and fluid turbulence. Consequently, the modeling only provides an approximation to combustion, but may, nonetheless, be adequate for purposes of engineering analysis.

The Kinetic Mechanism

The 16-species, 23-step mechanism, modified to eliminate the presure dependence of the rate constant in the first reaction, is presented in Appendix A at the end of this paper. The major changes to the mechanism, as given in Appendix B of Ref. 5, are:

i) The two-way reaction in Ref. 5 involving $CO + HO_2$ is replaced with a one-way global reaction involving N_2 as a catalyst, giving reaction 4 in the new mechanism

$$\{N_2\} + CO + HO_2 \rightarrow CO_2 + OH + \{N_2\}$$

where the brackets {} denote a third body.

ii) The reactions in Ref. 5 involving $N_2 + HO_2$ are modified to include the O-atom and OH-radical, giving reactions 3f and 3b

$$O + N_2 + HO_2 \rightarrow 2NO + OH$$
$$2NO + OH \rightarrow H_2 + HO_2 + O$$

where f and b refer to the forward and backward reactions, respectively.

iii) The reactions involving $2O \rightleftharpoons O_2$ in Ref. 10 are modified to include H_2 and N_2 as third bodies, giving reactions 5f and 5b

$$\{N_2\} + O_2 \rightarrow 2O + \{N_2\}$$
$$\{H_2\} + 2O \rightarrow O_2 + \{H_2\}$$

Furthermore, based on sensitivity analyses from the kinetics codes LSENS[6] and GLSENS,[7] other reactions are also modified. In addition to the reactions just cited, rate constants are modified on the first global reaction and several other reactions. In addition, the temperature coefficient, β, is modified on two reactions, and the concentration coefficients on several of the global reactions. The complete mechanism, with all constants, is given in Appendix A at the end of the text.

As previously stated, these modifications are made to eliminate the pressure dependence of the rate constant in the first, global reaction. This is achieved primarily through the addition of $\{N_2\}$ in reactions 4 and 5. These reactions together with reaction 14 are the rate-controlling reactions in this mechanism. The first reaction, i.e the fuel break-down step, is rate controlling only for cases that are very fuel lean.

The various constants in the reduced mechanism are derived by comparing results with the reduced mechanism to those from a detailed mechanism, obtained by combining the Jachimowsky mechanism for propane[8] with the nitrogen chemistry from Miller and Bowman.[9] The production of the O-atom and OH-radical for both a plug-flow and perfectly-stirred reactor using the LSENS code with the detailed mechanism and GLSENS for the reduced mechanism are compared. Furthermore, the rate constants are adjusted so that the reduced mechanism yields ignition-delay time that matches experimental data for both propane and Jet-A.[10]

Fig. 1-1 shows O-atom production for the reduced mechanism compared to the detailed mechanism for a plug-flow reactor. The results are obtained using GLSENS for the reduced mechanism and LSENS for the detailed mechanism. Fig. 1-2 shows the same for a well-stirred reactor. These cases represent the two theoretical limits for a combusting mixture. Ignition delay for Jet-A, as a function of ϕ and process pressure, calculated from GLSENS with the reduced mechanism is compared to experimental data in Fig. 2-1. There is close agreement over the range of equivalence ratios for this mechanism.

The Computer Code

The computer code used in this study is a version of KIVA-3[11] with two basic modifications: 1) a Reynolds-stress transport model for turbulence and 2) a chemistry routine that calculates forward and backward reaction rates from an input format whereby any set of kinetic reactions may be specified. Generally, the code was developed for computing two- and three-dimensional compressible flows, with combustion reactions, for gaseous or liquid-fuel sprays, in chambers of reciprocating piston engines. It is also well suited for through-flow combustors of the type in gas-turbine engines. The code solves the Reynolds-averaged transport equations with a time-marching scheme that is an arbitrary Lagrangian-Eulerian method with implicit continuous Eulerian modification for flows of low Mach Number. A semi-staggered grid is used whereby velocities are resolved on cell vertices and thermodynamic properties at cell centers. The governing equations are written in Cartesian coordinates and discretized by the finite-volume method. For cylindrical geometries, a wrapped-around grid and periodic boundary conditions are applied. A complete description of the code is given in Ref. 11.

A Reynolds-stress transport model is added in this version of KIVA-3, along with the k-ε model that came with the code. The Reynolds-stress model provides a higher-level turbulence formulation than the k-ε model, i.e. seven equations vs. two, giving a more complete description of the flow. It provides resolution of the turbulent momentum fluxes in the three normal and three transverse directions, along with the dissipation rate of the turbulence kinetic energy. It naturally includes effects of anisotropy, streamline curvature, sudden changes in strain rate, secondary motions, and flow rotation. The model employed is that of Speziale, Sarkar and Gatski,[12] denoted the SSG model after the authors, and recently employed by Yang in simulations of piston-engine combustion-chambers.[13] The model has been amply checked with simulations on experimental cases for non-reacting flows and has proven to give results for velocity fields that agree well with experimental data.[13] The formulation of this model is described in Ref. 13. In KIVA-3, the mean flow transport equations and the turbulence equations are solved sequentially, i.e. the Reynolds-stress equations are solved after resolution of the mean velocity from the momentum equations. This is the same procdeure used for the k-ε model. There is also a variant of the k-ε model in the KIVA-3V version of the code[14] that uses re-normalization group (RNG) theory, and includes the effects of compressibility by a rapid-distortion analysis. This turbulence model was used in modeling of the liquid-spray experimental case.

Premixed Propane Case

The first configuration modeled is a flame-tube experiment by Anderson.[15] The experiment consists of a premixed, propane-air mixture burned in an insulated, circular flow duct or flame tube,and stabilized by a multi-holed flame holder. The process pressure is 5.5 atm. The basic geometry and flow parameters for the experiment are listed in Table 1.

Table 1: Geometry & Flow Parameters

Diameter	10	cm
Overall Length	40	cm
From Flame Holder	30	cm
Inlet Gas/Air Velocity	32	m/s
Pressure	5.5	atm
Inlet Temperatures	600, 800	K
Equivalence Ratios	05 - 1.1	

The primary consideration of this experiment is measurement, by gas sampling, of NO concentrations in the combustion products at various locations along the axis of the flame tube. The case is modeled with the code by assuming axial symmetry and adiabatic walls. The multi-holed flame holder is modeled as a series of annular slots of constant width, except the slot nearest the wall which has a larger width.

The computed results of the NO emission index (EI, g of NO/kg of fuel) for this case are given in Fig. 2-2, where computed and experimental results are compared along the centerline of the flame tube for two inlet temperatures, 600 K and 800 K. The results are plotted against equivalence ratio. For the case of 800 K inlet temperature, two axial locations for the gas-sample probe are shown, 10 cm and 30 cm from the flame holder. The points for 600 K correspond to a sample-probe location for a 2 ms residence time of the combustion products. The experimental data is given by the dashed lines and the calculated values, by the solid lines.

Liquid Jet-A Experimental Injector

The second case modeled is a single fuel-injector, swirler module burning Jet-A fuel.[16] This module was tested in a combustion facility at Glenn Research Center where PLIF (planar laser induced fluoresence) measurements were made of relative OH concentrations in the region immediately downstream of the exit face. The module consists of a fuel nozzle, inner and outer air swirlers, and exhausts into a ceramic-lined plenum. The test plenum has quartz windows for making laser measurements. Fig. 3-1 shows the basic geometry, computational grid and laser-measurement area for this configuration. The fuel nozzle is located on the centerline. The geometry is axisymmetric. Flow parameters for this case are given in the following table:

Table2: Flow Parameters

Inlet Pressure	17	atm
Inlet Temperature	750	K
Air Flow Rate	0.186	kg/s
Swirler Inner Velocity	51	m/s
Swirler Outer Velocity	43	m/s
Swirl Number	1.17	
Module Δp	2	%
Spray Velocity	100	m/s
Spray Mean-Angle	10	deg
Spray Cant off CL	20	deg
Droplet Size40	μm	
Fuel Flow Rate	7.36×10^{-3}	kg/s
Equivalence Ratio	0.58	
Plenum Diameter	7	cm
Plenum Length	10	cm

The numerical simulation was done with the RNG turbulence model and marched for 90 k iterations to a quasi-steady state. Fig. 3-2 shows contours of OH concentrations from the numerical simulation, along with streamlines of the flow, throughout the plenum area. There is a circulation zone in the upper left corner of the plenum and a larger circulation region in the center where the flameholding and burning take place.

Fig. 3-3 shows the time-averaged, experimental PLIF images of OH over the laser-measurement area which extends from about 3 mm to 25 mm downstream of the module exit plane and about 54 mm in diameter,

centered on the axis of the plenum. Fig. 3-4 shows the computed results in approximately the same area. The PLIF images from the experimental data give relative levels of concentration and cannot be compared absolutely with the computed results. Only qualitative comparisons can be made. Along these lines, the region where the OH is present in the experimental and computed frames are of comparable location and shape, though the distribution of concentration levels is not entirely comparable. This, at least, indicates that the flame location from the numerical modeling is within reason. It should be noted that this is the near-field of the module exit surface, the area of highest uncertainty for flow-combustion modeling of liquid-spray combustion. Though gas-sample emission data is available for this case, the computational results over a range of inlet pressures and tempratures are not yet completed as of this writting.

Liquid Jet-A Annular Combustor

The third case modeled is a simple, annular, liquid-spray combustor configuration. For this case, the incoming flow passes over a bluff body that serves as a flameholder. There is a dilution-air slot, 1 cm wide, located on the inner and outer combustor liner and axially centered at 16 cm from the inlet plane. The outer diameter of the combustion chamber is 45 cm, and inner diameter, 15 cm. The combustor is 34 cm in length and necks down to a turbine nozzle at the out-flow plane. The computational domain is divided into 2352 computational cells and is an annular slice of one cell width, i.e. 2-D axisymmetric. Fig. 4-1 illustrates the configuration and the geometry is listed in Table 3:

Table 3: Geometry

Inlet Inner Radius	9	cm
Inlet Outer radius	21	cm
Flameholder Height	7	cm
Inner Casing Diameter	15	cm
Outer Casing Diameter	45	cm
Nozzle Outer Diameter	44	cm
Nozzle Inner Diameter	16	cm
Overall Length	34	cm
Computational Cells	2352	

Liquid Jet-A is sprayed into the air stream from a simple, hollow-cone fuel injector in an annular ring, with a 45° spray mean-cone angle and located at the center of the conical bluff body. Combustion is initiated by an ignition source which is simple heat addition to the fuel-air mixture for about 10 ms in an area between r = 12 & 18 cm and z = 10 & 20 cm as shown in Fig. 4-1.The simulation is done using the Reynolds-stress transport model for turbulence. The bluff body creates a circulation zone for flame holding as shown by the streamlines in Fig. 4-2. For simplicity, inner and outer walls are considered insulated, i.e. adiabatic. The spray break-up and evaporation models of the original KIVA-3 code are used. The inlet air velocity is about 30 m/s and the fuel-spray velocity, 100 m/s. The fuel flow rate is 1.5 kg/s which gives an equivalence ratio (ϕ) of about 0.54. The inlet pressure is about 25 atm. Table 4 lists the various flow parameters for this case.

Table 4: Flow Parameters

Inlet air velocity	30	m/s
Inlet pressure	25	atm
Inlet temperature	800	K
Dilution air	15	%
Spray velocity	100	m/s

Spray mean-angle	40	deg
Droplet diameter	20	μm
Fuel flow rate	1.5	kg/s
Equivalence ratio	0.54	

The transient history of the integrated temperature at the burner exit plane plotted against iteration number is given in Fig. 4-3. As indicated by the temperature history in Fig. 4-3, this case takes considerable time to reach quasi-steady state. After some initial transients through ignition and post ignition, the temperature reaches a steady mean-value of about 1300 K after about 100 k iterations. A profile of the quasi-steady temperature at 100k itrations is illustrated in Fig. 4-4. The burning occurs near the center of the annular area downstream of the bluff body and the peak temperature is of order 2360 K.

Normalized, average execution time and maximum memory for this case, run on a SGI Power Challenge system, R10000 CPU, 195 MHZ processor, are

Execution time	485	μs/cell/time step
Memory	2	GB

This case is somewhat hypothetical and no experimental data exists. Rather, a simple geometry is used to serve as a test of execution time and memory requirements for a combustor-like calculation. The computational results are shown primarily to demonstrate the utility of combining a Reynolds-stress turbulence model with the 16-species, 23-step mechanism for kinetics in application to a Jet-A, spray-combustor problem.

Conclusion

A 16-species, 23-reaction-step kinetics model for combustion of propane is demonstrated to give good results, in comparison to experimental measurements, for concentrations of NO in a premixed propane case. The mechanism is also applied to two cases with liquid Jet-A spray combustion. One case modeled an experimental injector-swirler module with computed results for OH concentrations compared qualitatively to PLIF measurements. The general shape of the OH regions are comparable for the computed and experimental results, but little more can be concluded. The utility of this mechanism is demonstrated on a UNIX workstation for a 2-D axisymmetric, liquid-spray combustor configuration. It should be noted that the code is basically explicit in handling the chemical reactions and species and, consequently, does not have the problem of large, stiff matrices characteristic of implicit codes with chemical reactions.

The intent is to continue testing the kinetic mechanism in the KIVA code with further modeling of experimental cases, particularly those with measured NO concentrations. Specifically, the experimental liquid-spray case will be analyzed over a range of inlet temperatures, presures and equivalence ratios, and compared with the measured NO concentrations.

Acknowledgement

The authors wish to acknowledge Yoland R. Hicks of the Glenn Research Center for the PLIF data taken on the experimental Jet-A spray combustion case.

References:

1. Giovangigli, V., and Smooke, M.D.: Reducing Mechanisms in *Reduced Kinetic Mechanisms and Asymptotic Approximations for Methane-Air Flames*, Lecture Notes Vol. 384 (Mitchell D. Smooke, Eds), Springer-Verlag, 1990.

2. Peters, N., ibid.

3. Rogg, B., ibid.

4. Kundu, K.P., Penko, P.F., and Yang, S.L.: Simplified Jet-A/Air Combustion Mechanisms for Calculation of NOx Emissions, AIAA 98-3986, July 1998.

5. Penko, P.F., Kundu, K.P., and Yang, S.L.: Application of a Reynolds-Stress Turbulence Model to Gas Turbine Combustor Calculations, AIAA 99-0485, January, 1999.

6. Radhakrishnan, K., and Bittker, D.A., NASA Reference Publication, 1329, February, 1994.

7. Bittker, D.A., NASA Reference Publication, 1362, March 1996.

8. Jachimowski, C.J., Comb. And Flame, Vol. 55, 1984, p. 213.

9. Miller, J.A. and Bowman, C.T.: Mechanism and Modeling of Nitrogen Chemistry in Combustion, Progress in Energy and combustion Science, Vol. 15, p.287, 1989.

10. Spadaccini, L.J., and TeVelde, J.A.: Autoignition Characteristics of Aircraft-Type Fuels, NASA CR-159886, June 1980.

11. Amsden, A.A.: KIVA-3: A Kiva Program with Block-Structured Mesh For Complex Geometries, LA-12503-MS, Los Alamos Laboratory, March 1993.

12. Turbulence model of Speziale et al.

13. Yang, S.L., Peschke, B.D., and Hanjalic, K.: IC-Engine Like Flow Study Using a Second-Moment Closure Model, ASME Paper 98-ICE-141, ICE Vol. 31-2, pp. 115-122, 1998.

14. Amsden, A.A.: KIVA-3V: A Block-Structured KIVA Program for Engines with Vertical or Canted Valves, LA-13313-MS, Los Alamos National Laboratory, July 1997.

15. Anderson, D.A., NASA TMX-71592, 1975.

16. Lee, C.M, et al.: Nitric oxide Formation in a Lean, Premixed-Prevaporized Jet A/Air Flame Tube: An Experimental and Analytical Study, NASA TM 105722, November 1992.

Appendix A. 16-Species, 23-Step Mechanism for Combustion of Propane and Jet-A in Air.

	Chemical Equation	A†	β	E‡
Global Reaction for Propane:				
1-P	$\{N_2\} + C_3H_8 \rightarrow 3CH + 5H + \{N_2\}$ a=0.8 b=0.8	4.50E+10	0.0	30,000.
Global Reaction for Jet-A:				
1-J	$\{N_2\} + C_{12}H_{23} \rightarrow 12CH + 11H + \{N_2\}$ a=0.8 b=0.8	5.50E+10	0.0	30,000.
Global Reactions Common to Propane and Jet-A:				
2f.	$\{CH\} + H_2 + N_2 \rightarrow 2NH + \{CH\}$ a=2.0 b=0.1 c=1.0	1.00E+16	0.0	78,000.
2b.	$\{CH\} + 2NH \rightarrow N_2 + H_2 + \{CH\}$ a=1.0 b=2.0	1.95E+15	0.0	53,900.
3f.	$\{O\} + N_2 + HO_2 \rightarrow 2NO + H + \{O\}$ a=0.1 b=0.5 c=1.0	1.95E+08	0.5	41,900.
3b.	$2NO + H \rightarrow N_2 + HO_2$ a=1.0 b=1.0	1.25E+10	0.0	6,000.
4.	$\{N_2\} + CO + HO_2 \rightarrow CO_2 + OH + \{N_2\}$ a=0.1 b=1.0 c=1.0	3.50E+13	0.0	22,934.
5f.	$\{N_2\} + O_2 \rightarrow 2O + \{N_2\}$ a=1.0 b=1.0	1.00E+18	0.0	122,239.
5b.	$\{H_2\} + 2O \rightarrow O_2 + \{H_2\}$ a=1.0 b=2.0	1.00E+18	0.0	0.
Kinetic Reactions Common to Propane and Jet-A:				
6.	$H_2 + OH \rightleftharpoons H_2O + H$	1.17E+11	1.3	3,626.
7.	$H_2 + O \rightleftharpoons H + OH$	2.50E+15	0.0	6,000.
8.	$H + O_2 \rightleftharpoons O + OH$	4.00E+14	0.0	18,000.
9.	$H_2 + 2H \rightleftharpoons 2H_2$	4.00E+20	-1.0	0.
10.	$H + O_2 \rightleftharpoons HO_2$	1.00E+15	-0.87	0.
11.	$H + HO_2 \rightleftharpoons H_2 + O_2$	1.50E+14	0.0	0.
12.	$O + HO_2 \rightleftharpoons OH + O_2$	2.50E+13	0.0	0.
13.	$CO + OH \rightleftharpoons CO_2 + H$	1.51E+07	1.30	-758.
14.	$\{N_2\} + 2CH \rightleftharpoons C_2H_2 + \{N_2\}$	1.00E+18	0.0	-758.
15.	$C_2H_2 + O_2 \rightleftharpoons 2CO + H_2$	3.00E+16	0.0	19,000.
16.	$CH + O \rightleftharpoons CO + H$	1.00E+12	0.7	0.
17.	$CH + OH \rightleftharpoons CO + H_2$	1.00E+13	0.0	0.
18.	$CH + NO \rightleftharpoons NH + CO$	1.00E+11	0.0	0.
19.	$N_2 + O \rightleftharpoons N + NO$	9.00E+13	0.0	75,000.
20.	$N + O_2 \rightleftharpoons NO + O$	6.30E+09	1.0	6,300.
21.	$NO + H \rightleftharpoons N + OH$	1.00E+12	0.0	0.
22.	$NH + O \rightleftharpoons NO + H$	2.50E+04	2.64	0.
23.	$NH + NO \rightleftharpoons N_2 + OH$	2.00E+15	-0.8	0.

The reaction rate is given by

$$R_f = A\, T^{\beta}\, e^{-(E/RT)}\, [X]^a\, [Y]^b\, [Z]^c$$

Unless otherwise specified, a, b, and c are the stoichiometric coefficients: $aX + bY + cZ \rightarrow \ldots$

Footnotes:

† Units are cm-sec-mole-cal-Kelvins.

‡ Units are cal/mole.

In reactions 2 , 3 and 8: f is the forward reaction, and b, the backward reaction.

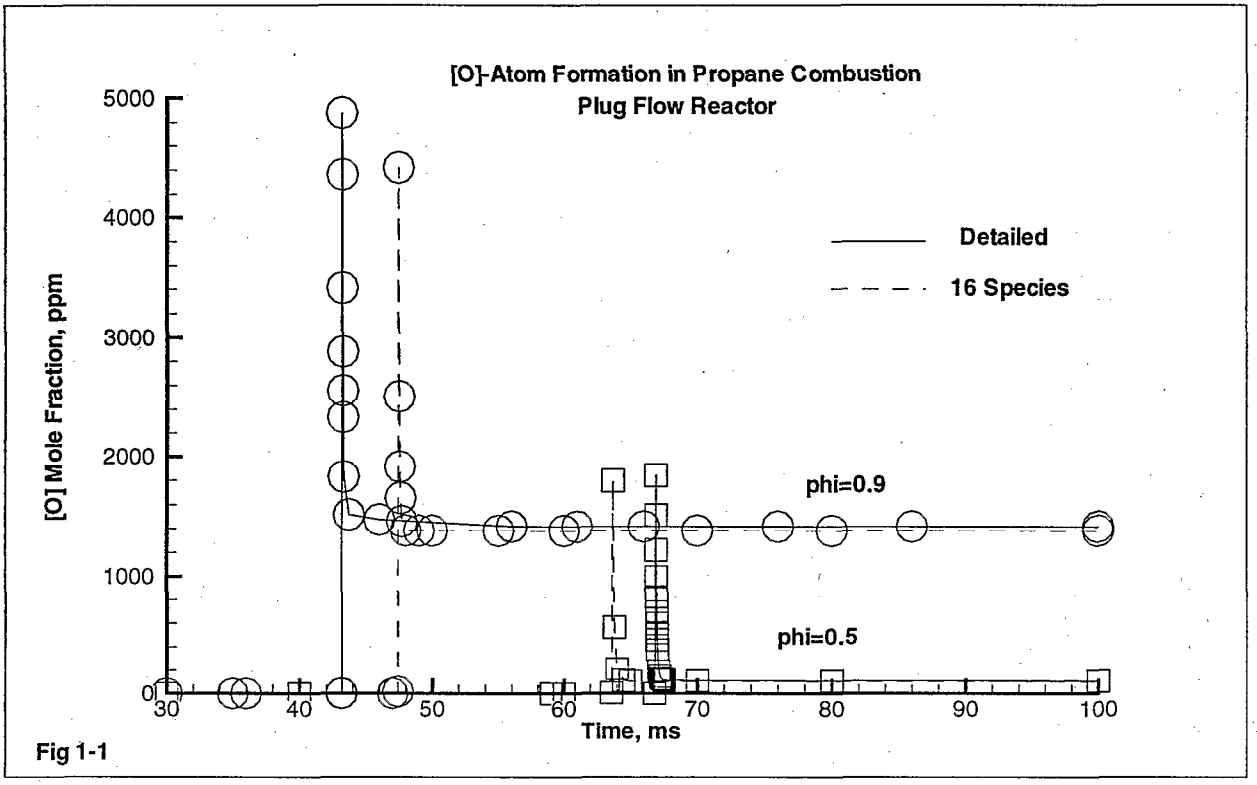

Fig 1-1

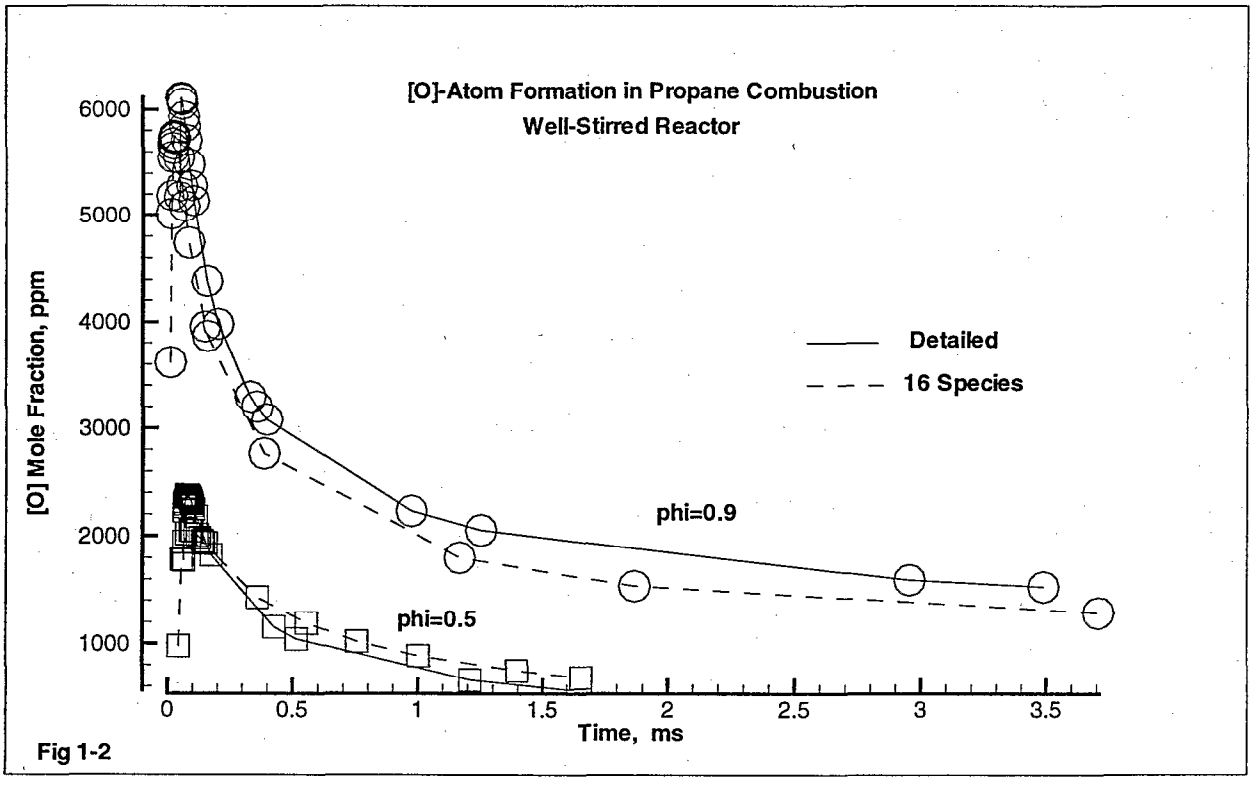

Fig 1-2

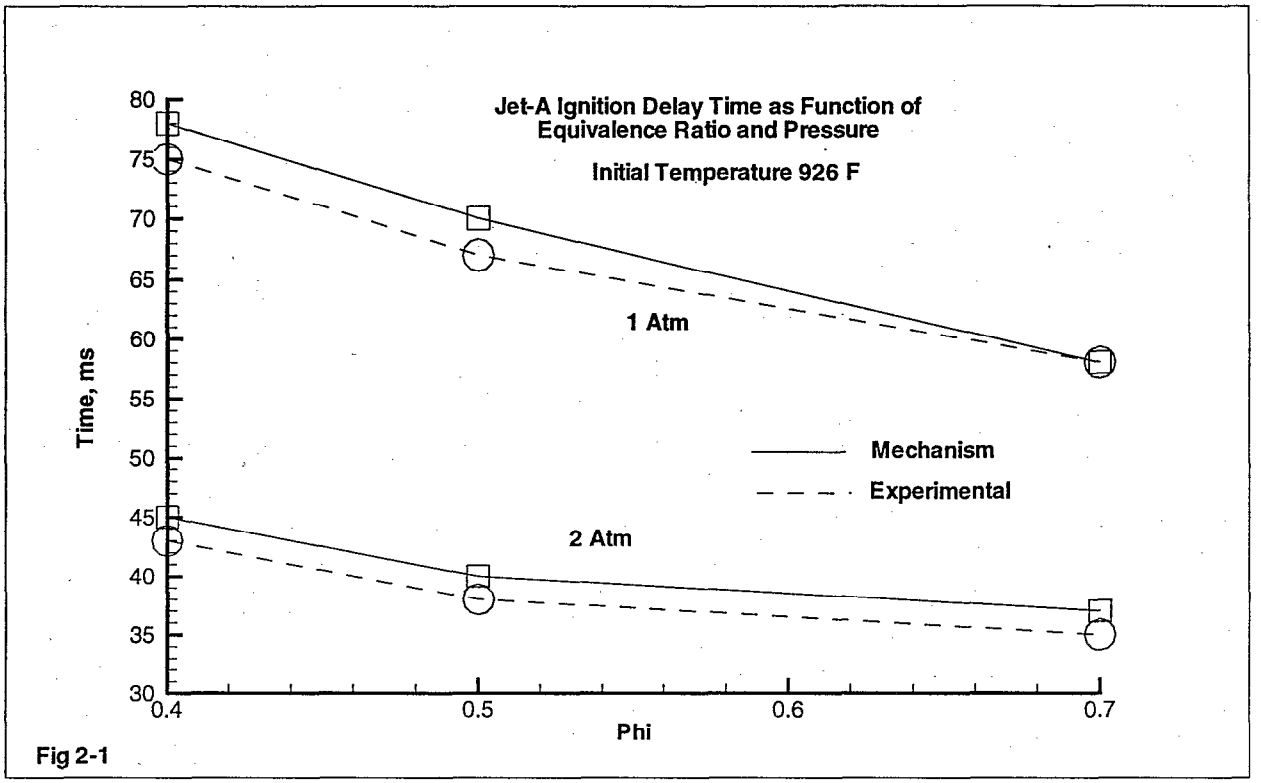

Fig 2-1

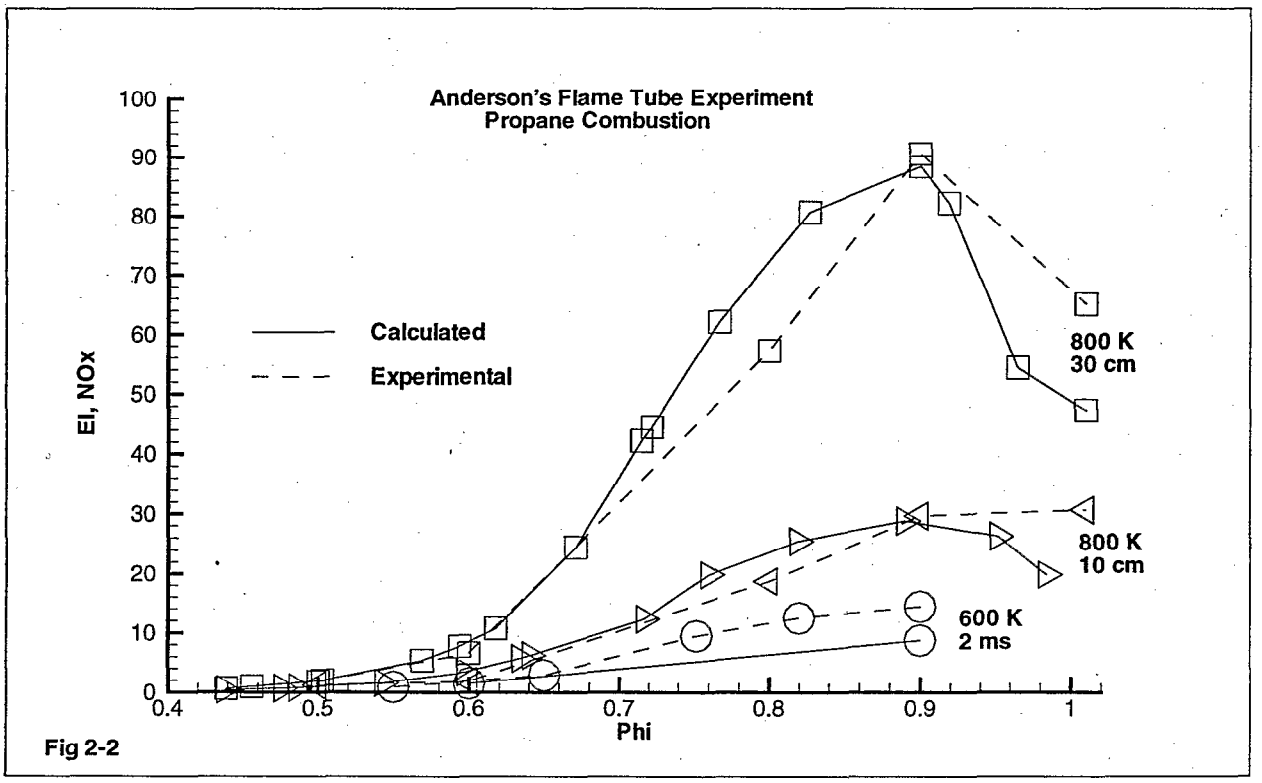

Fig 2-2

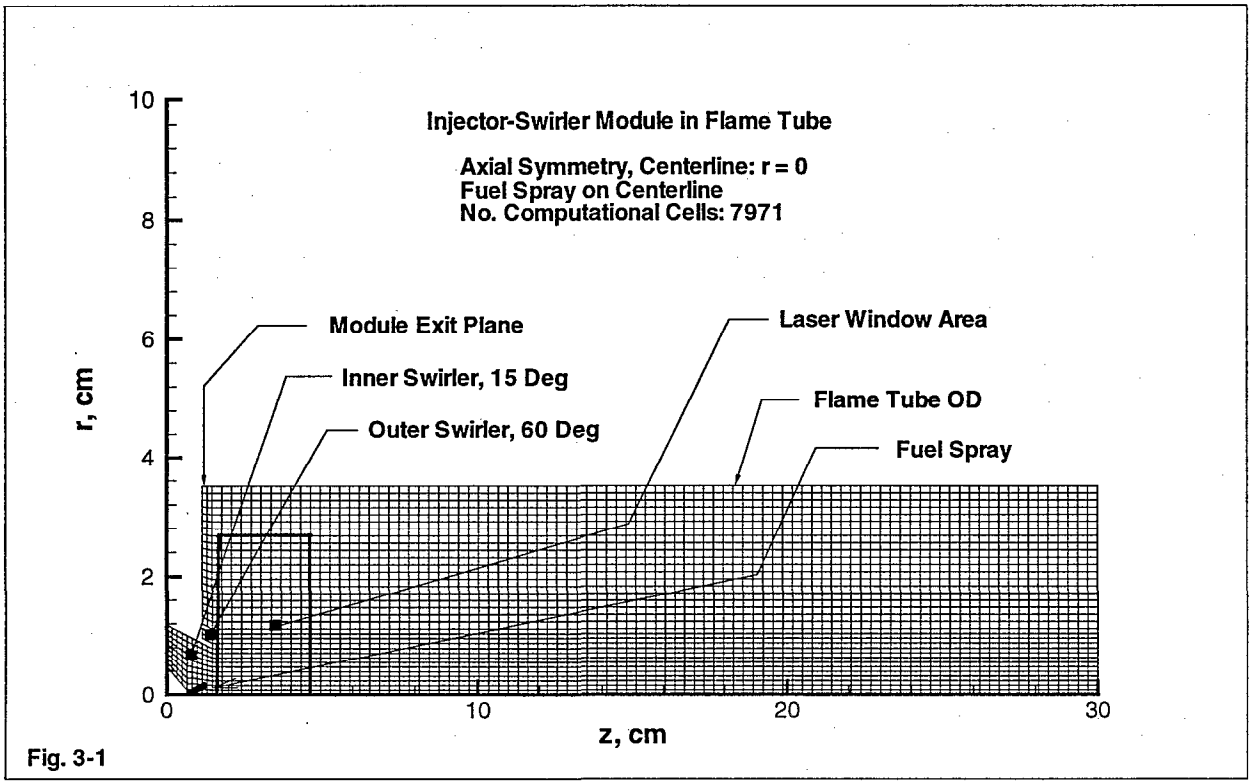

Fig. 3-1

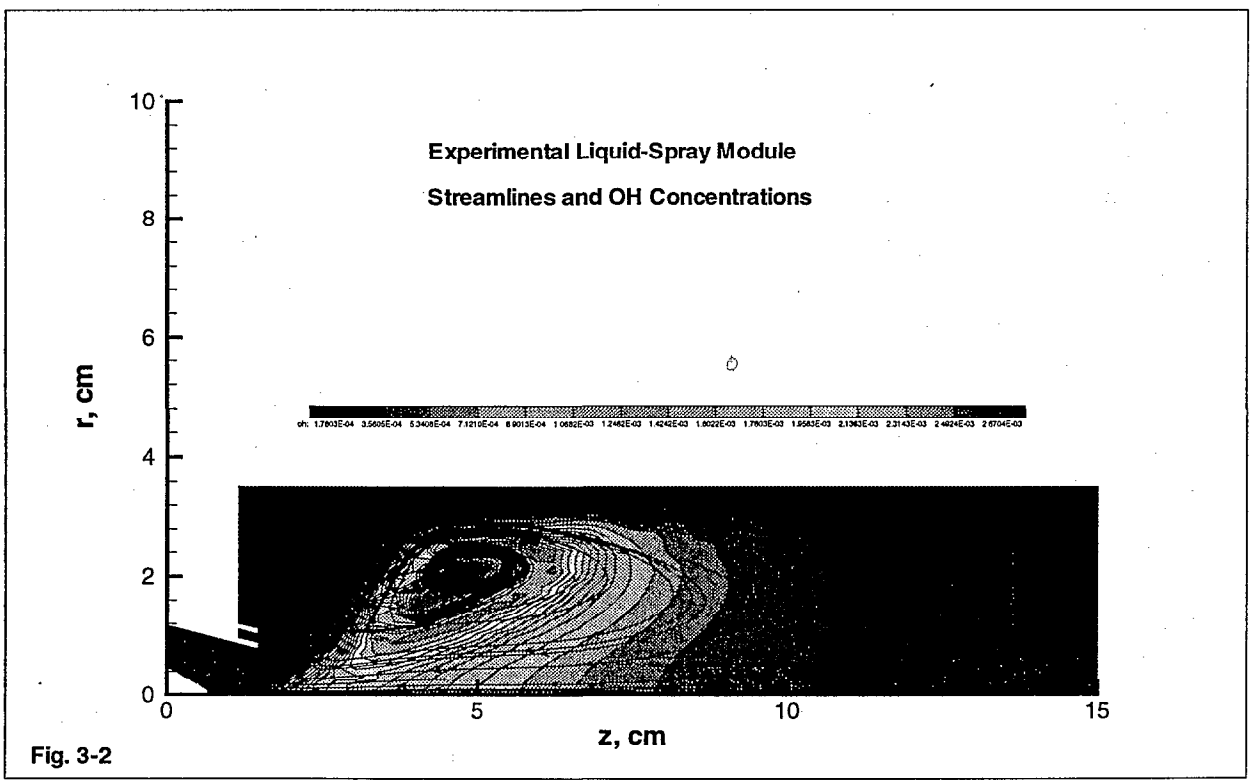

Fig. 3-2

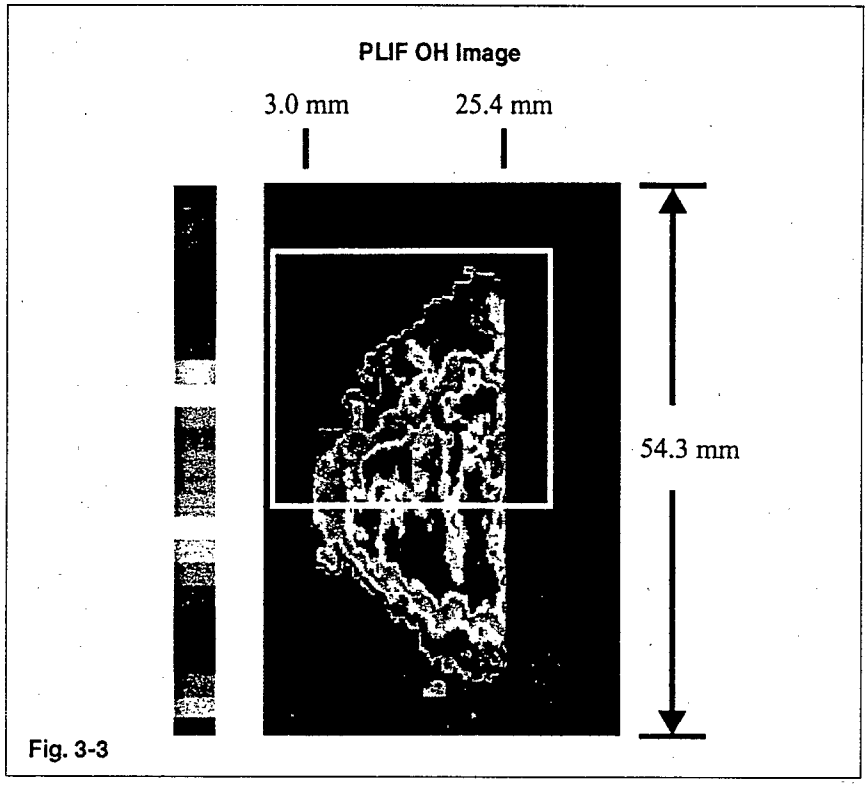

Fig. 3-3

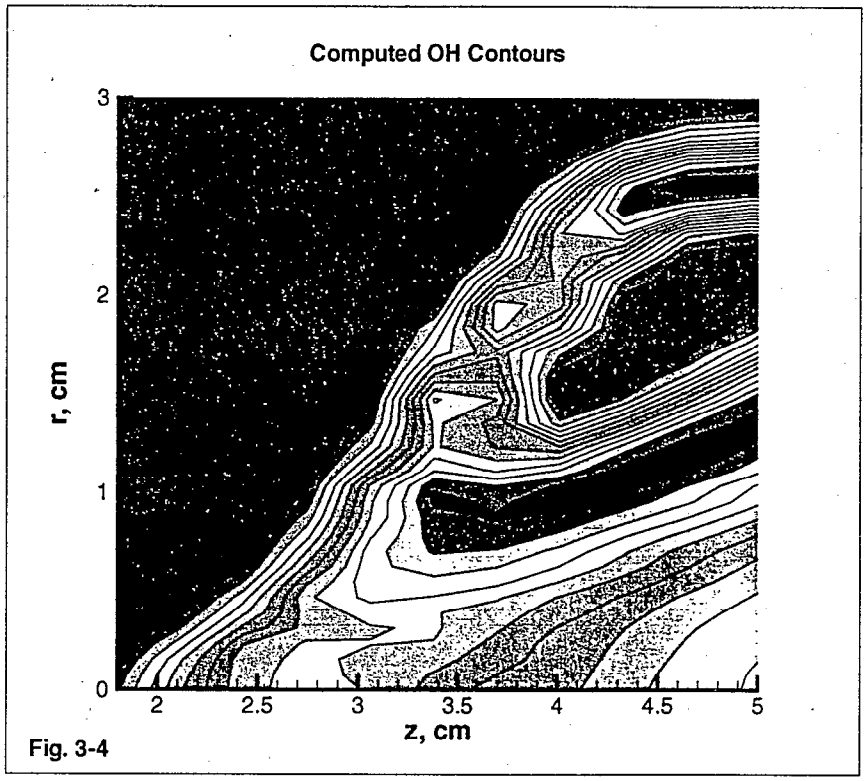

Fig. 3-4

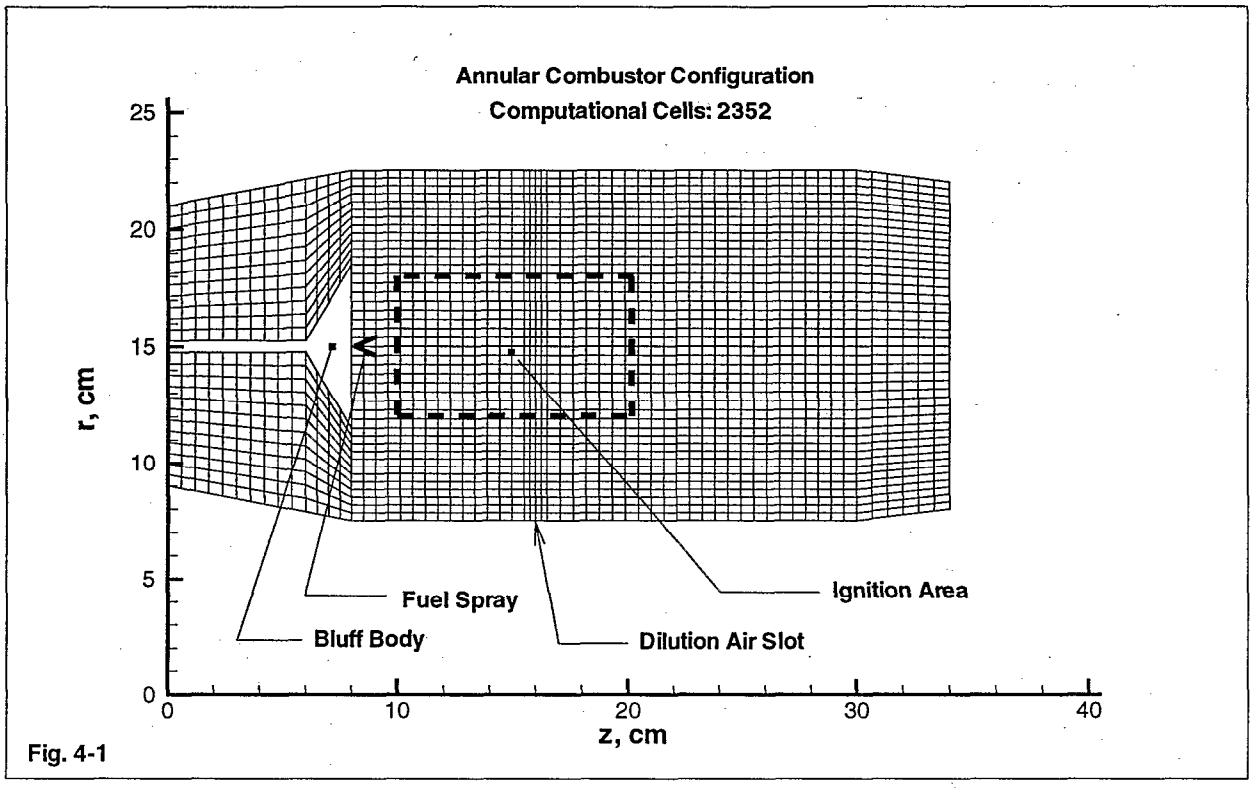

Fig. 4-1

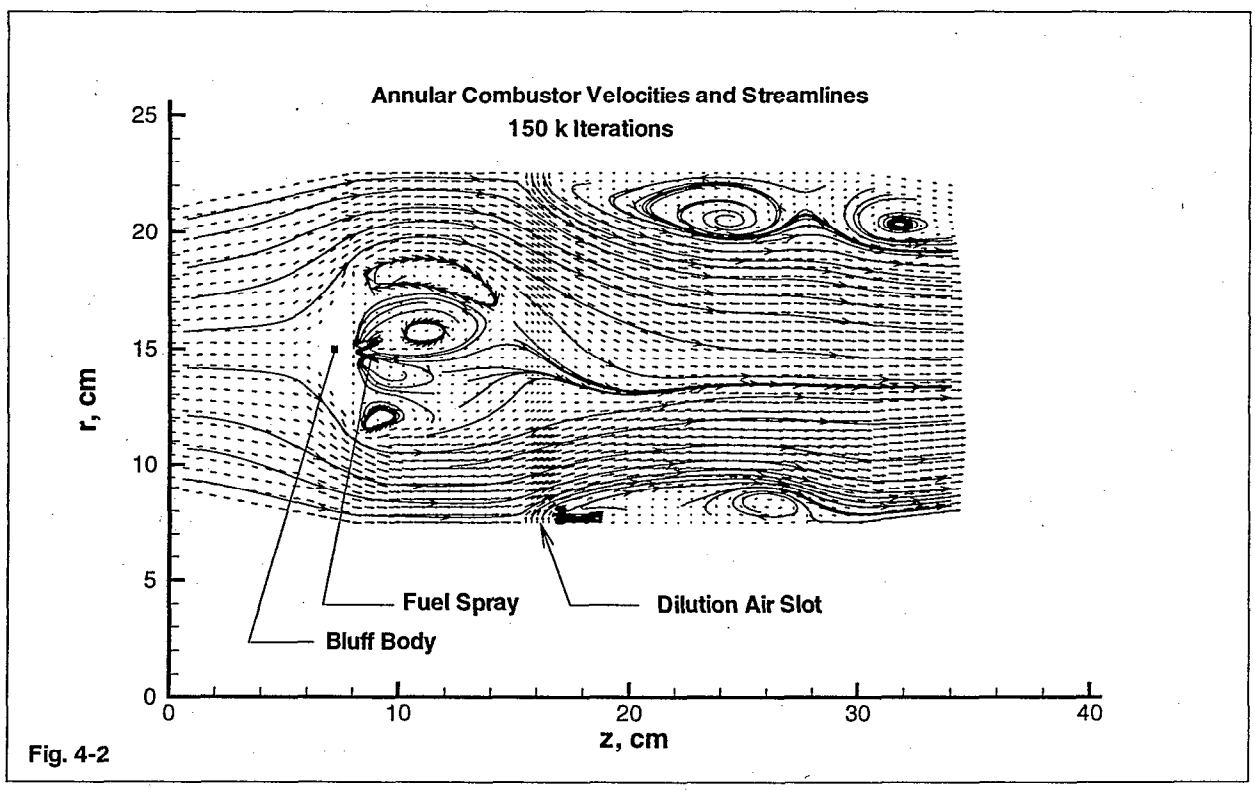

Fig. 4-2

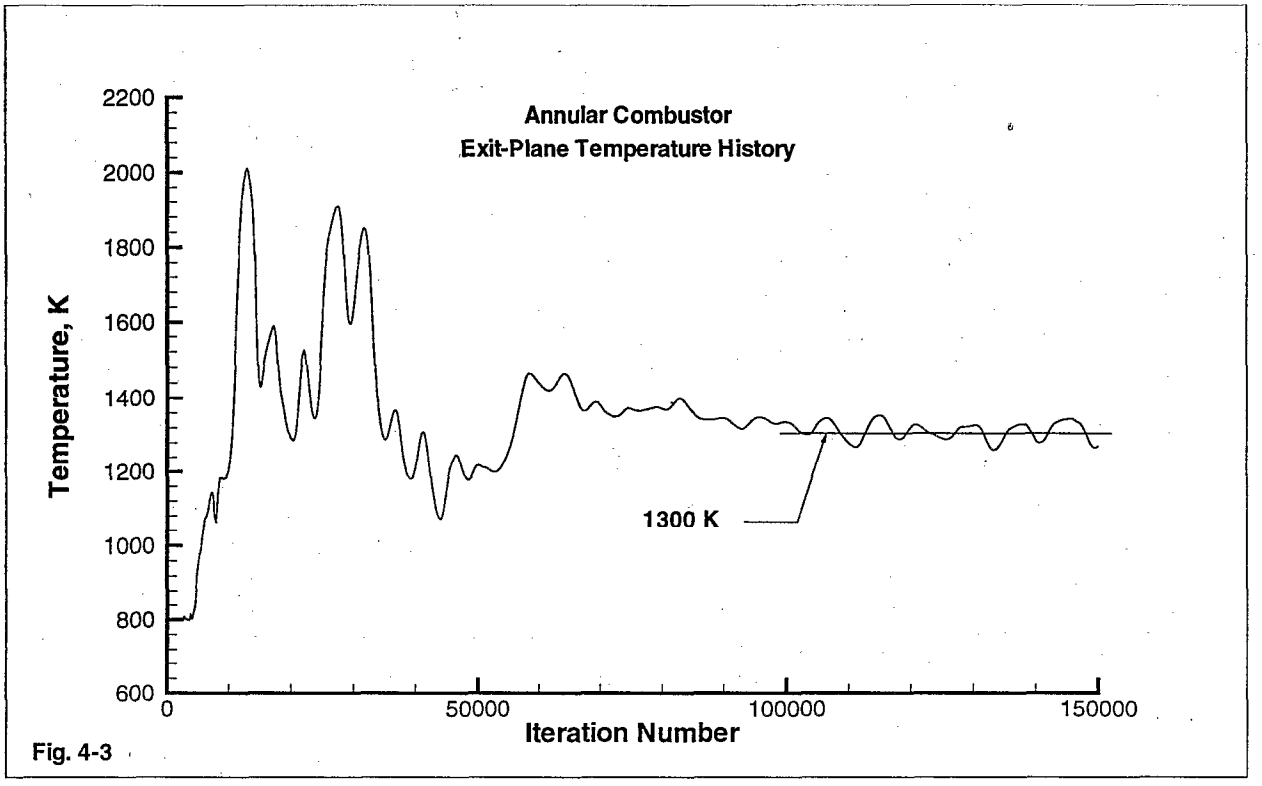

Fig. 4-3

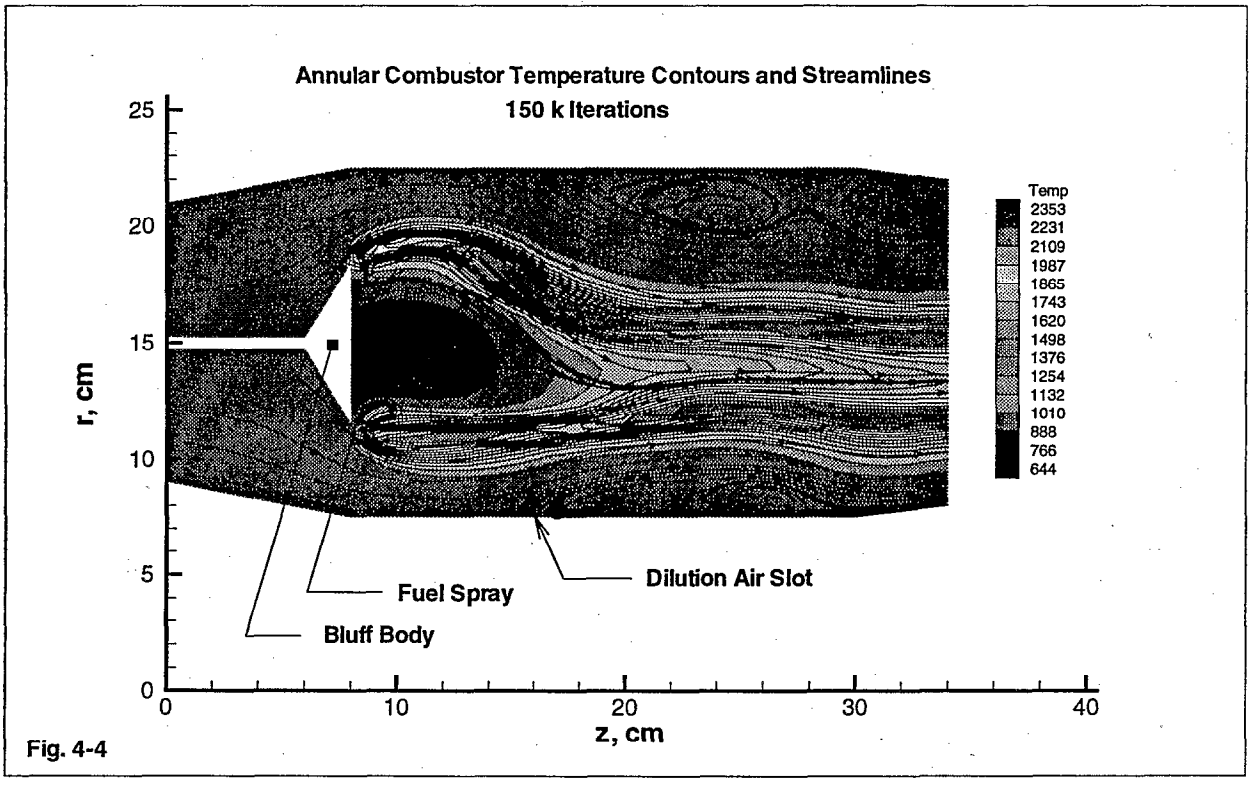

Fig. 4-4